Eur. Phys. J. D **45**, 17–23 (2007)
DOI: 10.1140/epjd/e2007-00208-4

THE EUROPEAN PHYSICAL JOURNAL D

Study of heavy nuclei at FLNR (Dubna)

Yu.Ts. Oganessian[a]

Flerov Laboratory of Nuclear Reactions (JINR), 141980 Dubna, Moscow region, Russia

Received 15 November 2006
Published online 27 June 2007 –

Abstract. Experiments are described and main results presented on the synthesis and decay properties of superheavy nuclides, produced in fusion reactions induced by a ^{48}Ca-beam on heavy actinide targets. In such reactions neutron-rich nuclei are formed. For them, according to theory, an abrupt enhancement of stability due to nuclear shell effects is expected. The decay properties of the new nuclides are compared with calculations of theoretical models, which predict the existence of "islands of stability" in the region of hypothetical superheavy elements.

PACS. 25.60.Pj Fusion reactions – 27.90.+b $220 \leq A$

1 Introduction

It is well-known that the main field of application of the macroscopic, liquid drop (LD) model has been the description of the average properties of the nuclear masses and deformation energies. From the analysis of the detail properties of heavy nuclei it had become obvious that the macroscopic approaches needed corrections by means of the shell model [1,2]. The main achievements of the macro-microscopic theory are connected with the development of the calculation method of these corrections to the nuclear ground and highly deformed states [3]. The concept of nuclear shells is here defined as large-scale non-uniformity in the energy distribution of the individual particle states near the Fermi energy [4], directly connected to the nuclear binding energy. In such a way, the model corrects the energy according to the nuclear structure (effect of nuclear shells, paring), based on the calculation of the nuclear levels [5,6].

In many publications (e.g., see the reviews [4,7–12] and references therein), a number of the existing disagreements between the macroscopic model and experiment were explained by taking into account the shell effect when calculating the nuclear energy. One important consequence of these calculations was the disclosure of a significant gap in the spectrum of low lying levels in the region of hypothetical superheavy nuclei, viz. a new (following $N = 126$) closed spherical neutron shell $N = 184$. It was also shown that the considerable variations of the binding energy of spherical nuclei were due to the nuclear shells, and that shell effects might be present also in deformed "magic nuclei" (deformed shells). And finally, at further and quite significant increase of the deformation arising in fission, *the shell effects continued to play an important role* in defining the potential energy and the nuclear inertial masses. Other, purely microscopic self-consistent approaches to the description of nuclear binding energies, also predict significant increase of the binding energy of heavy nuclei at $N \approx 162$ and $N = 184$. The theoretical predictions for the new shells, which in fact are not too far from the well established region of the actinides (it is a question of nuclei with mass ∼280–300), push far away the limits of nuclear masses and extend the region of existing elements at least as far as $Z \sim 120$ and even more.

Of main interest to us are the basic consequences of these models from the point of view of their experimental verification, and this is the main purpose of the present talk. The remarkable success in the past few years achieved in the synthesis of heavy nuclei in cold fusion reactions are related basically to isotopes in the vicinity of the $N = 162$ shell, mainly at $N < 162$. The decay properties (α-decay energies and half-lives, as well as spontaneous fission half-lives) of practically all synthesized nuclei up to the heaviest one (^{277}112) are well explained by model calculations reflecting the effect of the deformed shells $Z = 108$ and $N = 162$. But in order to probe the effect of the next, spherical shells, which influence a much wider charge and mass region of heavier nuclei, it is necessary to synthesize nuclei with $Z \geqslant 114$ and $N \geqslant 172$. This is hard to achieve in cold fusion reactions. One of the key questions pertains to the production of new "magic" nuclei in heavy-ion induced reactions.

[a] e-mail: oganessian@jinr.ru

2 Reactions of synthesis

In the standard fusion theory, tested in many experiments with light projectiles (from ^{4}He to ^{26}Mg), the evaporation-residues (EVR's) cross section, $\sigma_{EVR}(E_x) = \Sigma\ \sigma_{xn}(E_x)$, is determined by the cross section for the formation of the compound nucleus with excitation energy E_x and by the probability of its survival, $P_{xn}(E_x)$, during de-excitation by emission of x-nucleons (for the heavy nuclei — mainly neutrons) and γ-rays: $\sigma_{xn}(E_x) = \sigma_{CN}(E_x)P_{xn}(E_x)$.

It is then assumed that for all collisions with $\ell \leqslant \ell_{crit}$, fusion (amalgamation of the interacting nuclei) takes place automatically in a very short time after overcoming the Coulomb barrier. Indeed, if the nuclear attractive force was stronger than the Coulomb repulsion, this simple fusion pattern would be quite defensible. It has been shown also that when the two magic nuclei ^{208}Pb and ^{48}Ca fuse the maximum cross sections for evaporation residues are reached with low excitation energy (cold fusion) and small number of evaporated neutrons ($x = 1$–3) [13] Since 1974 the cold fusion reactions ^{208}Pb, ^{209}Bi + massive projectile ($A_P \geqslant 50$) have been used in the synthesis of the heaviest elements. When the projectile becomes more and more heavy, the excitation energy of the compound nuclei decreases (down to $E_x \approx 15$–10 MeV) and the transition to the ground state takes place by the emission of only one neutron and γ-rays [14–16]. As a result, the survivability of the compound nucleus $P_{xn}(E_x)$ significantly increases, this being the main advantage of the cold fusion reactions.

Another peculiarity of cold fusion reactions of the nuclei ^{208}Pb or ^{209}Bi with stable isotopes from ^{54}Cr to ^{70}Zn as projectiles lead to the formation of compound nuclei with small neutron excess. The EVR's are some 10–15 mass units shifted from the β-stability line. This, in turn, leads to a considerable decrease in their half-lives. Finally, in cold fusion reactions the six heaviest elements with $Z = 107$–112 were synthesized (see also RIKEN experiment on the synthesis of element 113 [17]). As can be seen from Figure 1a, the cross section $\sigma_{1n}(Z_{CN})$ — of the main channel of the synthesis reaction — exponentially decreases with the increase of Z_{CN}. When Z_{CN} changes from 102 to 113 the cross section decreases by almost a factor of 10^7. The observed strong decrease in the cross section with the increase of Z_{CN} in cold fusion is evidence that strong obstacles arise on the way of formation of the cold compound nucleus itself.

Obviously, the mechanism of fusion of massive nuclei, such as ^{208}Pb and ^{70}Zn, significantly differs from the above-considered simple scenario of formation of compound nuclei using light projectiles. The exchange of nucleons at the contact point and the following formation of a composite system of summed mass are far from guaranteeing its evolution to a more compact shape near the ground state. This transition is the result of a complex collective motion of the system in conditions of strong Coulomb repulsion. Now, the process of formation of the EVR's takes place via three stages: capture — motion along the collective trajectory — survival; the resulting cross section is $\sigma_{EVR} = \sigma_{capt}P_{dyn}P_{sur}$. Transport models, describing the stage of collective motion in different assumptions about the dynamical properties of the nuclear system, indicate a strong decrease of P_{dyn} with the increase of the proton number.

In order to decrease the factors hindering fusion, it is desirable to make use of more asymmetric reactions, and to obtain an increase in the neutron number of the EVR's by using both target and projectile nuclei with maximum neutron excess. As target material, it is reasonable to use neutron-rich isotopes of the actinides (Act.), such as ^{244}Pu, ^{248}Cm and ^{249}Cf, produced in high-flux reactors and thus having largest neutron excess. Among the projectiles, undoubted advantage has the doubly magic nucleus of the rare isotope ^{48}Ca. The compound nucleus ^{292}114, produced, for example, in the fusion of ^{244}Pu and ^{48}Ca, acquires 8 additional neutrons compared to the case of the ^{208}Pb + ^{76}Ge cold fusion reaction.

These 8 neutrons, as will be shown below, play a key role in the production and the decay properties of superheavy nuclei. Compared to the cold fusion reaction ^{208}Pb + ^{76}Ge ($Z_PZ_T = 2624$), the Coulomb repulsion in the reaction ^{244}Pu + ^{48}Ca ($Z_PZ_T = 1880$) decreases by almost 40%, which, in turn, should lead to the decrease of the factors hindering the formation of a compound nucleus. On the other hand, due to the magic structure of ^{48}Ca, the excitation energy at the Coulomb barrier $E_x^{\min}$ of the compound nucleus ^{292}114 amounts to approximately 30 MeV, a value by 10–15 MeV lower than in typical hot fusion reactions induced by lighter projectiles.

The last stage — the survival of the compound nucleus — is the decisive one in the given method of synthesis of the heaviest nuclei. The estimations of $E_x^{\min}$ and the following experiments, aimed to measure the excitation functions for evaporation products, have shown that the compound nuclei with $Z_{CN} = 112$–118, may attain excitation energy from 30 to 55 MeV. This energy will be released by a cascade emission of 2 to 5 neutrons (the evaporation of charged particles is significantly less probable) and γ-rays. Indeed the excitation functions correspond to the evaporation mainly of 3 or 4 neutrons from the excited nucleus, the maximum cross sections for evaporation residues are observed at $E_x \approx 40$ MeV [18] (hot fusion). The cross sections of nuclei with $Z = 102$–110, produced in the $4n$-evaporation channel of the fusion reactions Act. + ^{22}Ne, ^{26}Mg, ^{36}S($5n$), are presented in Figure 1b (the neutron number of the corresponding compound nuclei is shown on the horizontal axis). Neutron number of the corresponding compound nuclei is shown on the horizontal axis). Since there is no significant hindrance for fusion in such mass-asymmetric reactions ($Z_PZ_T = 920$–1500), the strong decrease in the cross section σ_{4n} is connected mainly with the survivability of the nuclei. The relatively high production cross section of isotopes with $Z \leqslant 105$ is a consequence of the high fission barrier, which is almost completely determined by the shell effect of the two closed neutron shells $N = 152$ and $N = 162$. At neutron numbers $N_{CN} > 162$, as can be seen from Figure 1b (lower graph) the fission probability significantly increases with the decrease of B_f. However, if the predictions of the theoretical models (see above) about the existence of the next

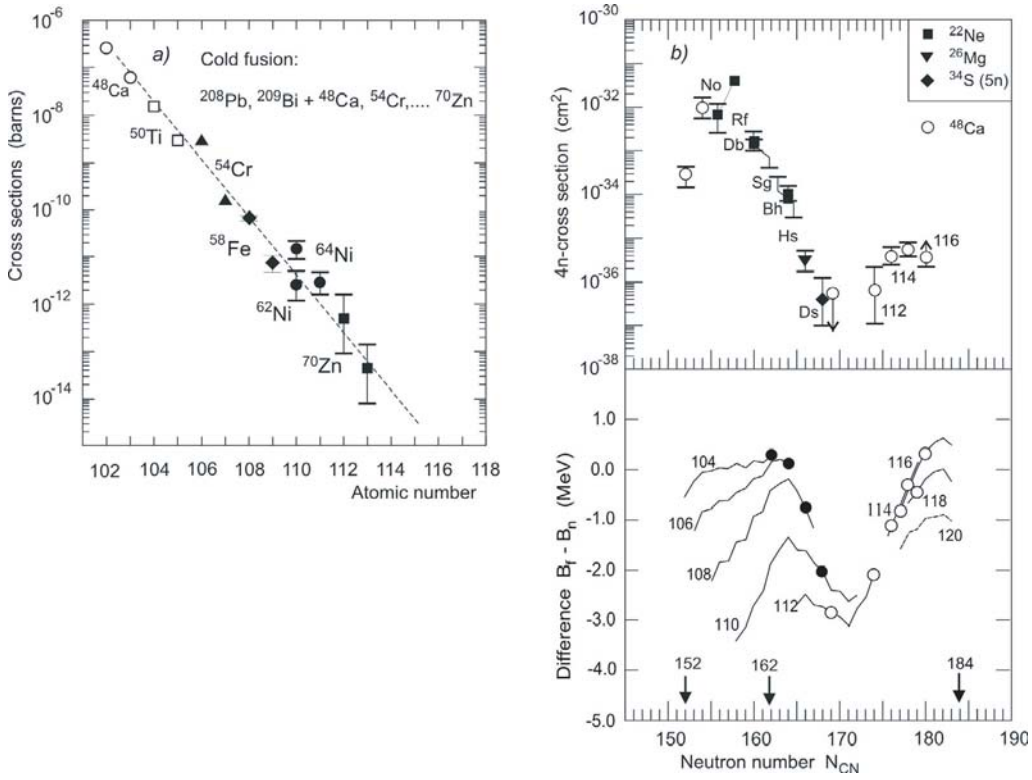

Fig. 1. (a) Maximal cross sections of the $1n$-evaporation channel in cold fusion reactions. (b) Upper panel: experimental cross sections at the maximum of $4n$-evaporation channels in hot fusion reactions. Lower panel: calculated values of $(B_n - B_f)$ for isotopes of elements 102–120 with different neutron number.

closed shell $N = 184$ is justified, the fission barrier height will again increase when advancing to the region where $N_{CN} \geqslant 174$ and $Z_{CN} \geqslant 112$. In turn, the nuclear survivability will increase too and as a result, one can expect even a rise in the σ_{EVR} for heavy nuclei with large neutron excess. Indeed, as can be seen from the experimental data presented in Figure 1b, when increasing the number of neutrons from $N_{CN} = 169$ (^{233}U + ^{48}Ca) to $N_{CN} = 172$ (^{237}Np + ^{48}Ca) and then to $N_{CN} = 178$–180 (^{244}Pu, ^{248}Cm + ^{48}Ca), σ_{EVR} grows by more than one order of magnitude. For this reason, the observed increase in the survivability of the excited nuclei with neutron number appears to be, to our opinion, evidence for the existence of the closed neutron shell in the region of $N \geqslant 180$.

3 Setting the experiments

The Gas-Filled Recoil Separator (DGFRS) used in the experiments with ^{48}Ca-projectiles is schematically presented in Figure 2. The calculated and measured in the test experiments transmission efficiency of the separator for $Z = 112$–118 nuclei is about 35–40% [19], whereas full-energy ^{48}Ca projectiles, projectile-like ions, and target-like nuclei are suppressed by factors $\sim 10^{17}$, 6×10^{14}, and 10^4–10^6, respectively.

The typical beam intensity of ^{48}Ca-ions at the target was 1.0–1.2 pμA. The consumption of the ^{48}Ca material amounted to about 0.5 mg/h. In the experiments, targets of actinide oxides of the highly enriched isotopes of U, Np, Pu, Am, Cm and Cf (thickness of $\approx$0.35 mg/cm^2) were used.

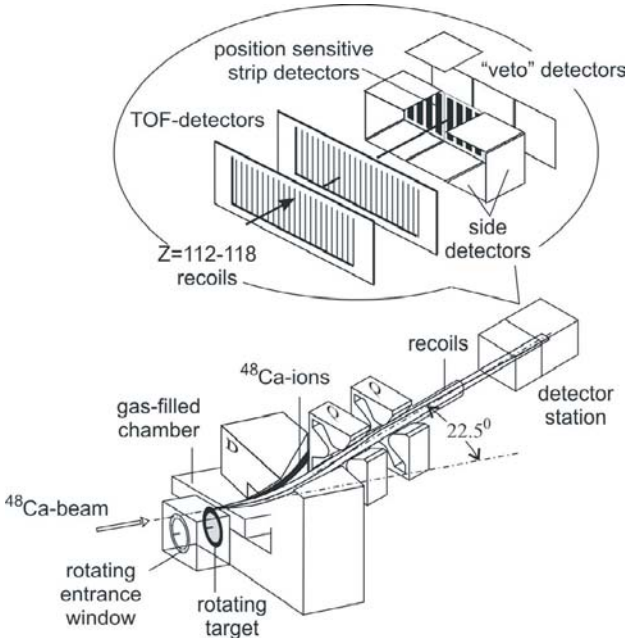

Fig. 2. Layout of the gas-filled recoil separator.

EVRs passing through the separator were implanted in a 4×12-cm^2 semiconductor detector with 12 vertical position-sensitive strips. The detection efficiency of the focal-plane detector array for α-particles is 87% of 4π; for detection one fission fragment — close to 100%, for two fission fragment — about 40%. For α-particles, emitted by the parent or daughter nuclei, it is possible to choose wide

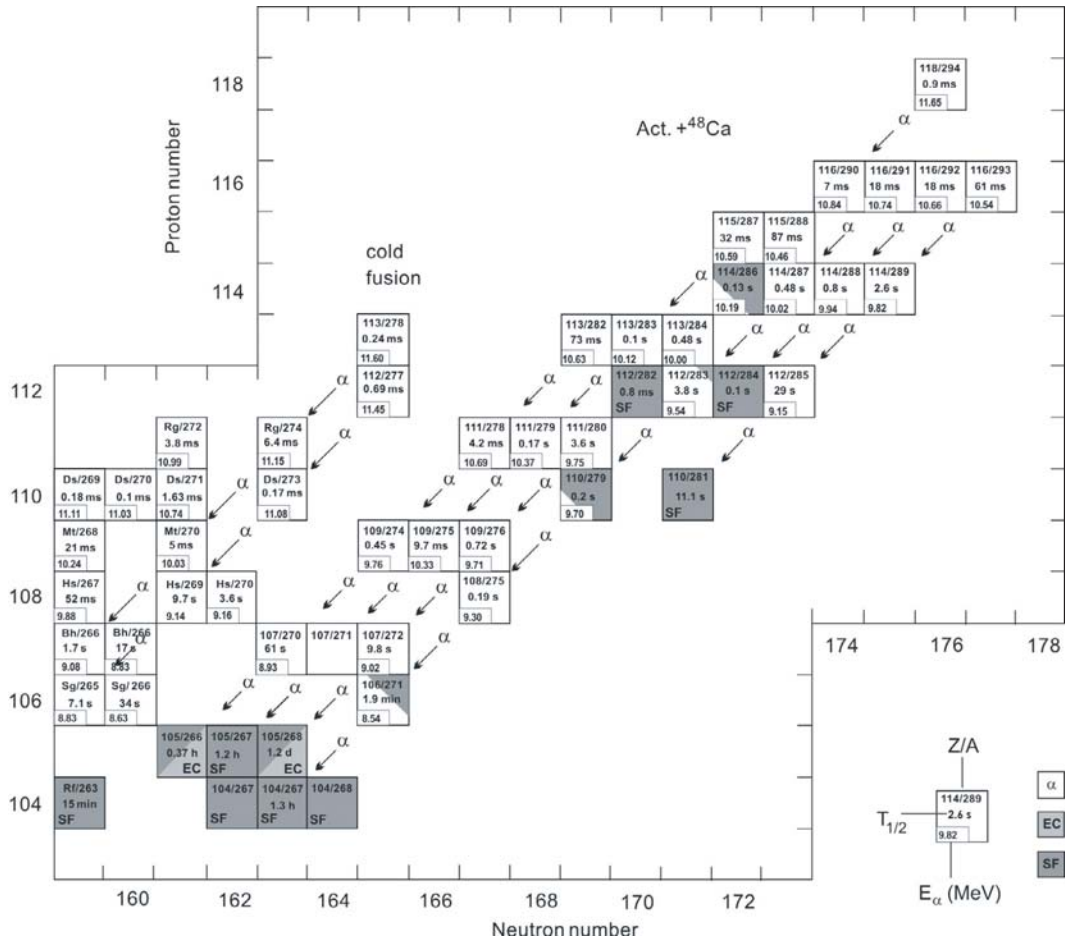

Fig. 3. Chart of the heaviest nuclides. The squares contain the half-lives (without errors) and the maximum α-transition energy (E_α in MeV).

enough energy and time gates $\delta E_{\alpha 1}$, $\delta t_{\alpha 1}$ and $\delta E_{\alpha 2}$, $\delta t_{\alpha 2}$ and employ a special low-background detection scheme. An example: during the irradiation of the ^{243}Am-target, the beam was switched off after a recoil signal was detected with parameters of implantation energy and *TOF* expected for evaporation residues, followed by an α-like signal with an energy in the interval $\delta E_{\alpha 1}$ in the same strip/position and a time interval $\delta t_{\alpha 1}$ of up to 8 s. If the first α-particle was not detected (the probability being about 13%), then the switching off the beam was done when a second α-particle in the corresponding $\delta E_{\alpha 2}$ and $\delta t_{\alpha 2}$ intervals was detected. At the registration of the second α-particle the beam-off period is extended to 12 min, whereas of the third — to 3 h.

Such running condition allowed detection of rare events and decay characteristics of heaviest nuclei with decay time of up to 1 d and even longer [20]. The most short-lived nuclei are detected in DGFRS corresponding to $t \geqslant 5$ μs. In this way, the setup allows investigation of nuclei in a wide range of half-lives — from 10^{-5} s to more than 10^5 s.

From the characteristics of the DGFRS, which are given above, it follows that with a ^{48}Ca-beam intensity of 1.2 pμA, 0.35 mg/cm^2 target thickness and a beam dose 5×10^{18} (realized for 200 h of operation) the observation of one decay event corresponds to the production cross section of about 0.7 pb.

4 Experimental results

For the synthesis of superheavy nuclei at DGFRS, the fusion reactions of ^{48}Ca with target nuclei, the isotopes of U, Np, Pu, Am, Cm and Cf (9 isotopes of six actinide elements), were used. The decay chains are presented in Figure 3. In the investigations carried out at different ^{48}Ca energies, 29 new nuclides (34 including preliminary data for the decay chain of ^{282}113) were detected, all of them being evaporation products and their daughter nuclei in the region of $Z = 104 \div 118$ and $A = 266 \div 294$ [18,21].

The identification of the atomic numbers of the nuclides was performed by:

- the mechanism of fusion reactions (excitation functions and cross bombardments ensuring variation of the proton and neutron numbers of the compound nucleus);
- the decay properties of the nuclei in the decay sequences (half-lives T_α and α-decay energies Q_α of even-even (and for many even-odd) isotopes; see Figure 4;

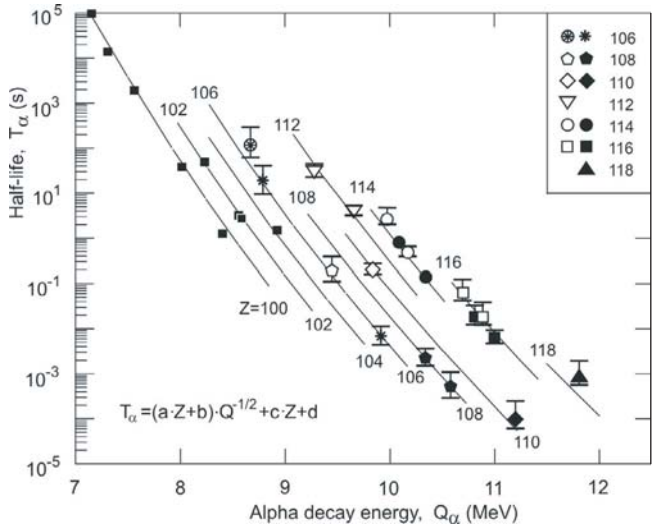

Fig. 4. Half-lives T_α as a function of the α-decay energy Q_α for nuclei with even atomic numbers $Z \geqslant 100$ (indicated in the figure). The solid lines represent calculations using the Viola-Seaborg formula (given in the figure). The black symbols denote even-even isotopes, the open symbols — even-odd.

– the radiochemical identification of the atomic number of the nuclides ^{268}Db and ^{283}112 – links of the decay chains of the parent nuclei: ^{288}115 and ^{291}116 [22,23].

All methods give the same identification of the atomic number of the synthesized nuclei. When the atomic numbers of the parent nuclei are determined (showing that they are the products of *xn*-evaporation channels), the identification of the mass of an isotope comes to the quantification of evaporated neutrons at various excitation energies. This is achieved:

– by means of the measured excitation functions ensuring variation of the neutron number in the compound nucleus;
– by producing the same nuclei in different ways: as evaporation residues and as α-decay products of heavier nuclei.

The adjoining four isotopes of the elements with $Z = 112$, 114 and 116, genetically connected with the daughter nuclei by consecutive α-decays give a self-consistent picture of the atomic and mass numbers of all nuclides, synthesized in the ^{48}Ca-induced experiments. Further verification of the identification of the mass number of the isotopes follows from the decay properties. Because of the high suppression of spontaneous fission of nuclei with odd neutron numbers, their decay chains are longer and the total decay time is noticeably higher than in the neighbouring even-N isotopes (see chains on the Fig. 3).

4.1 Alpha decay

As can be seen from Figure 3, the odd isotopes of element 112 and all isotopes (even and odd) with $Z \geqslant 113$ predominantly undergo α-decay. As known from the theory of α-decay, in this case the probability for the decay (or the half-life T_α) is directly connected to the decay energy Q_α and the atomic number of the nucleus. The experimental values obtained earlier in hot and cold fusion reactions and belonging to the α-decay of even-even nuclei with $100 \leqslant Z \leqslant 110$ with new data for all isotopes with even proton numbers from $Z = 106$ to 118, produced in ^{48}Ca-induced reactions, are shown in Figure 4. The experimental values Q_α(exp) and T_α(exp) shows steep raise of the T_α with increase the neutron number in heaviest nuclei. They can be used for the calculation of the atomic numbers of nuclei comprising the chains of correlated decays. For example the probability that the consecutive α-transitions observed in the ^{245}Cm, ^{248}Cm + ^{48}Ca reaction take place in the nuclei with atomic numbers $116 \rightarrow 114 \rightarrow 112 \rightarrow 110$ amounts to 0.992.

The values of Q_α(th), obtained in the framework of the MM-model in the version of [24] for the isotopes of all elements with even atomic numbers from $Z = 100$ to 118 and with odd atomic numbers from $Z = 103$ to 115, are presented in Figures 5a and 5b, respectively. The predicted Q_α(th) values for the heaviest nuclei, observed in our experiments are systematically larger than the experimental data.

At the same time, the trends of the predictions are in good agreement for the 23 nuclides with $Z = 106$–118 and $N = 165$–177. The trend of the $Q_\alpha(N)$ systematics, predicted by theory and confirmed by experimental data can be considered *as direct evidence for the deformed neutron shell closure at* $N = 162$.

The comparison of Q_α(exp) with the values Q_α(th), calculated within the Skyrme-Hartree-Fock-Bogoliubov (HFB) and the Relativistic Mean Field models (RMF), was carried out, too. In the HFB model a better agreement is obtained with masses from [25] calculated with 18 parameters. Finally, in the RMF model the agreement between theory and experiment is least satisfactory. But it cannot be excluded that a better agreement can be achieved in this model also by using a different set of parameters.

As a whole, the measured values of Q_α(exp) are in agreement with theory, because the model calculations do not claim to be more precise in determining Q_α(th) than 0.4–0.6 MeV. We must recall, that all three models predict the same spherical neutron shell at $N = 184$, but different proton shells, $Z = 114$ (MM) and $Z = 120$, 124 or 126 (HFB, RMF). Yet, all describe the experimental data equally well. Such insensitivity with respect to the various models in this region of Z and N can be explained either by the remoteness of the nuclei under consideration from the closed shell at $N = 184$ or by the weaker influence of the proton shells at $Z = 114$ or higher, compared to that of the neutron shell at $N = 184$.

4.2 Spontaneous fission

For 8 out of the 34 synthesized nuclei spontaneous fission is the predominant mode of decay. In two more nuclei, ^{271}Sg

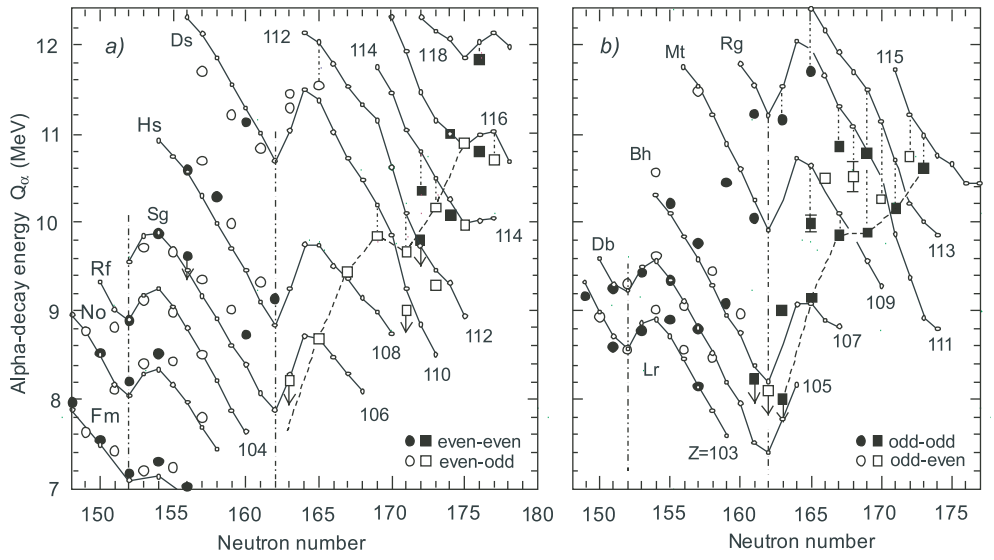

Fig. 5. Alpha-decay energy vs. neutron number for: (a) the isotopes of even-Z elements with $Z \geqslant 100$, (b) isotopes of odd-Z elements with $Z \geqslant 103$. Squares correspond to the nuclei, produced in ^{48}Ca-induced reactions. Dashed lines are long sequences of correlated decays of the nuclei $^{288}115$ and $^{291}116$. The solid lines are Q_α(th), calculated in the MM-model.

and $^{286}114$, spontaneous fission competes with α-decay. For the remaining nuclides spontaneous fission was not observed. The partial SF half-lives of nuclei with $N \geqslant 163$, produced in fusion reactions with ^{48}Ca, together with the half-lives of SF-nuclides with $N \leqslant 160$, are shown in Figure 6. Four isotopes of element 112 with $N = 170$–173 are located in a region, where a steep rise of $T_{SF}(N)$ is expected. Indeed, in the even-even isotopes $^{282}112$ and $^{284}112$ the difference of two neutrons increases the partial half-life T_{SF} by two orders of magnitude. The neighbouring odd isotopes $^{283}112$ and $^{285}112$ undergo α-decay. For them, only lower limits of T_{SF} can be determined (shown in the figure). Such a picture is observed also for the even-even isotopes of element 114: the additional two neutrons in the nucleus $^{286}114$ ($T_{SF} \approx 0.13$ s) lead to significant increase of the stability relative to spontaneous fission. It is significant that the rise of stability relative to spontaneous fission is observed for the nuclei are by 10–12 neutrons away from the closed neutron shell $N = 184$.

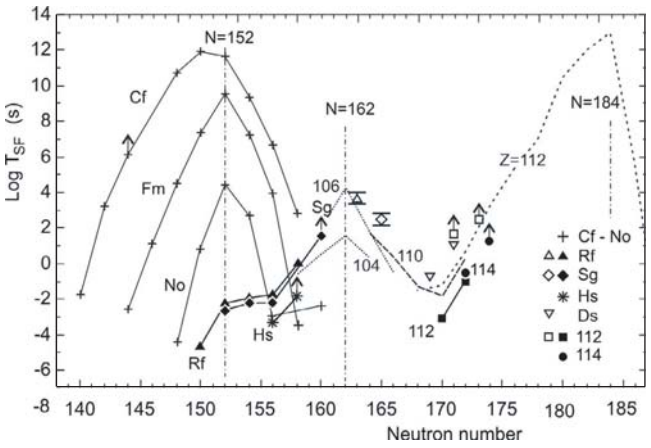

Fig. 6. Partial half-lives for spontaneous fission T_{SF} vs. N for nuclei with even $Z = 98$–114. Solid symbols and crosses denote even-even nuclei, open symbols — even-odd. Solid lines are drawn through the experimental points of even-even nuclei, the dashed lines — calculated T_{SF}(th).

On moving to the nuclei with $Z < 110$ and $N < 170$ the probability for spontaneous fission decreases again when the close deformed shell $N = 162$ is approached. The stabilizing effect of the $N = 162$ shell manifests itself in the properties of the even-even isotopes of Rf, Sg and Hs with $N \leqslant 160$, which, as seen from Figure 6, are well described by the mentioned model calculations. The odd SF-isotopes with $Z = 104$–110, produced in the ^{48}Ca-induced reactions, are located in the transition region, where the larger the neutron number, the smaller the effect of the $N = 162$ shell. In this region, the $N = 184$ shell comes into effect. Such a behaviour of T_{SF}(exp) as a function of Z and N correlates with the SHE fission barrier heights and has been predicted by all models: MM, HFB and RMF. For the isotopes of element 115, due to the strong hindrances to spontaneous fission of nuclei with odd proton (or/and neutron) number, α-decay predominates as far as the $N = 162$ shell, where, similarly to the previous case, the sequences terminates by spontaneous fission.

The decay properties of the nuclei obtained in Act. + ^{48}Ca reactions show that the basic theoretical concept on the existence of closed shells in the region of the hypothetical superheavy elements and their decisive role in defining the limits of nuclear mass has received its experimental confirmation.

The experiments were performed at U-400 heavy ion cyclotron of the FLNR (JIINR) in collaboration with Analytical and Radiochemical Division of LLNL (USA).

References

1. O. Haxel, J.H. Jensen, H.E. Suess, Phys. Rev. **75**, 1766 (1949)
2. M.G. Mayer, Phys. Rev. **75**, 1969 (1949)

3. V.M. Strutinski, Nucl. Phys. A **95**, 420 (1967); V.M. Strutinski, Nucl. Phys. A **122**, 1 (1968)
4. M. Brack et al., Rev. Mod. Phys. **44**, 320 (1972)
5. S.G. Nilsson et al., Nucl. Phys. A **131**, 1 (1969)
6. B. Mottelson, S.G. Nilsson, Phys. Rev. **99**, 1615 (1955)
7. A. Sobiczewski, F.A. Gareev, B.N. Kalinkin, Phys. Lett. **22**, 500 (1966)
8. H. Meldner, Ark. Fys. **36**, 593 (1967)
9. U. Mosel, W. Greiner, Z. Phys. **222**, 261 (1969)
10. P. Möller, J.R. Nix, J. Phys. G **20**, 1681 (1994)
11. A. Sobiczewski, Phys. Part. Nucl. **25**, 119 (1994)
12. W. Greiner, Int. J. Mod. Phys. E **5**, 1 (1995)
13. S. Hofmann, Rep. Prog. Phys., **61**, 639 (1998)
14. G.N. Flerov et al., Nucl. Phys. A **267**, 359 (1976)
15. P. Armbruster, Annu. Rev. Nucl. Part. Sci. **35**, 135 (1985)
16. G. Munzenberg, Rep. Prog. Phys. **51**, 57 (1988)
17. S. Hofmann, G. Munzenberg, Rev. Mod. Phys. **72**, 733 (2000)
18. K. Morita et al., J. Phys. Soc. Jpn **73**, 2593 (2004)
19. Yu.Ts. Oganessian et al., Phys. Rev. C **69**, 054607(2004); Yu.Ts. Oganessian et al., Phys. Rev. C **70**, 064609 (2004)
20. K. Subotic et al., Nucl. Instr. Meth. A **481**, 71 (2002)
21. Yu.Ts. Oganessian et al., Phys. Rev. C **69**, 021601(R) (2004)
22. Yu.Ts. Oganessian et al., J. Phys. G **34**, R165 (2007)
23. S.N. Dmitriev et al., Mendeleev Commun. **1**, 1 (2005)
24. R. Eichler et al., Nature **442**, 47 (2007)
25. I. Muntian, Z. Patyk, A. Sobiczewski, Acta Phys. Pol. B **34**, 2073 (2003); I. Muntian, Z. Patyk, A. Sobiczewski, Phys. At. Nucl. **66**, 1015 (2003)
26. S. Goriely et al., Phys. Rev. C **66**, 024326 (2002)